Role of the Putative Transmembrane Segment M3 in Gating of Neuronal Nicotinic Receptors†

Antonio Campos-Caro,‡,§ José C. Rovira,§,|| Francisco Vicente-Agulló,‡ Juan J. Ballesta,|| Salvador Sala,⊥ Manuel Criado,‡ and Francisco Sala*,||

Departamento de Neuroquímica, Departamento de Farmacología, Departamento de Fisiología, and Instituto de Neurociencias, Universidad de Alicante, Apartado Correos 374, 03080 Alicante, Spain

Received September 17, 1996; Revised Manuscript Received December 30, 1996⊗

ABSTRACT: The involvement of some structural domains in the gating of the neuronal nicotinic acetylcholine receptor (AChR) was studied by expressing functional α7/α3 chimeric subunits in *Xenopus* oocytes. Substitution of the M3 transmembrane segment in the α7 subunit modifies the kinetic properties of the chimeric AChRs as follows: (a) a 6-fold reduction in the maximal current evoked by nicotinic agonists, (b) a 10-fold decrease in the macroscopic desensitization rate, (c) an increase of almost 1 order of magnitude in the apparent affinity for acetylcholine and nicotine, and (d) a decrease in the affinity for α-bungarotoxin. Computer simulations showed that the first three effects could be accounted for by a simple kinetic model in which chimeric AChRs presented a smaller ratio of the gating rates, β/α, and a slightly slower desensitization rate. It is concluded that the M3 domain influences the gating of neuronal AChRs.

Nicotinic acetylcholine receptors (AChR)[1] are members of the superfamily of ligand-gated ion channels (LGICs), which are found at the neuromuscular junction and throughout the central and peripheral nervous systems [for recent reviews, see Papke (1993), Edmonds et al. (1995), McGehee and Role (1995), and Karlin and Akabas (1995)]. A chemical signal, generated by the binding of two molecules of acetylcholine (ACh) to the extracellular binding sites of AChRs, must be transmitted to the channel gate located some distance away. There is a number of reports involving different structural domains in the gating properties of AChRs and other LGICs, including residues located at the N-terminal domain (O'Leary & White, 1992; Aylwin & White, 1994; McLaughlin et al., 1995; Chen et al., 1995; Figl et al., 1996), the M1 domain (Lo et al., 1991), the M2 domain (Revah et al., 1991; Akabas et al., 1992; Filatov & White, 1995; Labarca et al., 1995), the M2−M3 loop (Rajendra et al., 1995), and the M4 domain (Lee et al., 1994). Most of them have been performed in *Torpedo* or muscle type AChRs, and though their conclusions may be extended to other LGICs, there is a relative lack of information concerning neuronal AChRs.

Recently, by using α7/α3 chimeric constructs, we have described the contribution of a single charged residue located at the M2−M3 loop in coupling agonist binding to opening of the channel of neuronal AChRs (Campos-Caro et al., 1996). Interestingly, two of those chimeras, C10 and C21 (see Figure 1), exhibited very different functional properties when compared with the α7 wild type (WT) receptors. This

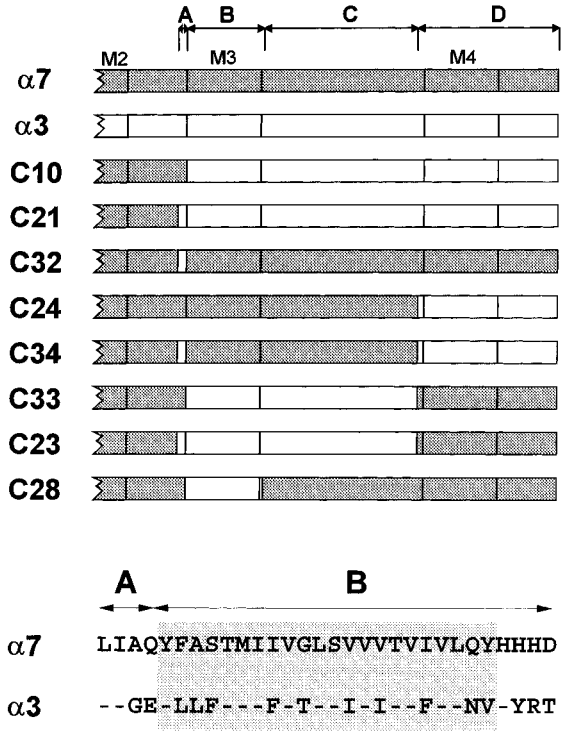

FIGURE 1: (Top) Schematic diagrams of α7/α3 chimeras. The color codes for the sequences of α7 and α3 subunits are displayed in the first two rows (gray for α7 and white for α3). Since all chimeras share the α7 sequence in the N-terminal part, only the domains swapped are depicted for the sake of clarity. These domains include (A) two residues in the M2−M3 loop, (B) the M3 segment, (C) the M3−M4 intracellular loop, and (D) the M4 segment and C-terminal region. (Bottom) Alignment of residues in domains A and B of the α7 and α3 subunits. Residues postulated to be within the M3 segment are on the shaded area.

† This work was supported by Grants GV-2535/94 from Generalitat Valenciana, PB92−0346 from The Ministry of Education of Spain (DGICYT), and SCI*CT91−0666 from the Commission of the European Community.

* Author to whom correspondence should be addressed : Francisco Sala, Departamento de Farmacología, Universidad de Alicante, Apdo. Correos 374, 03080 Alicante, Spain. Telephone: +34-6-590-3904. Fax: +34-6-590-3905. E-mail: fsala@ua.es.

‡ Departamento de Neuroquímica.

§ Equal contributors.

|| Departamento de Farmacología.

⊥ Departamento de Fisiología and Instituto de Neurociencias.

⊗ Abstract published in *Advance ACS Abstracts,* February 15, 1997.

[1] Abbreviations: AChR, nicotinic acetylcholine receptor; ACh, acetylcholine; LGIC, ligand-gated ion channel; α-Bgt, [^{125}I]-α-bungarotoxin.

S0006-2960(96)02348-3 CCC: $14.00

suggested that new domains could be involved in gating. Therefore, we decided to study in more detail the role of these domains in the gating of AChRs. We present evidence which indicates that the putative transmembrane segment M3 may be involved in such a process. Our results are compatible with a simple kinetic scheme where the M3 domain modifies the gating rate constants (α and/or β) and, to a lesser extent, the desensitization rate.

MATERIALS AND METHODS

Construction of Chimeras. Bovine nicotinic α3 and α7 sequences (Criado et al., 1992; García-Guzmán et al., 1995) were used to construct chimeric subunits, which were made by performing two successive PCR amplifications, as described (Hertlize & Koenen, 1990; García-Guzmán et al., 1994).

Oocyte Expression. Chimeric DNAs were inserted into the pSP64T vector (Krieg & Melton, 1984). Capped mRNA was synthesized in vitro using SP6 RNA polymerase. Defoliculated Xenopus oocytes were injected with 5 ng of mRNA in 50 nL of sterile water, and measurements were made within 3−6 days after injection.

Electrophysiological Recordings. Whole membrane currents were measured with a two-electrode voltage-clamp amplifier at room temperature (22−25 °C). In order to avoid the presence of contaminating calcium-activated chloride currents, all oocytes were incubated for 3−4 h in Barth's storage media containing 100 μM BAPTA-AM, the membrane permeant form of the Ca chelator bis(2-aminophenoxy)ethane *N*,*N*,*N*',*N*'-tetraacetate (BAPTA). Latter experiments with chimeric subunit C28 and its WT control were made after injection to each oocyte of 40 nL of a BAPTA-containing solution as described (Galzi et al., 1992). After either of these procedures, we found no evidence of secondary chloride currents, as no biphasic currents were detected upon cholinergic stimulation at any holding potential (Séguéla et al., 1993). Kinetic measurements were not significantly affected by removal of oocyte vitelline membranes (not shown). Oocytes were perfused with frog Ringer solution containing (in millimolar) 115 NaCl, 2.5 KCl, 1.8 $CaCl_2$, and 10 HEPES (pH 7.2). Nicotinic agonists were applied during 1−3 s through a 1.5 mm diameter pipette located close to the oocyte. Currents were filtered at 50 Hz by an eight-pole Bessel filter, digitized at 250 Hz, and stored on a hard disk for later analysis. Data were acquired by a DigiData 1200 interface driven by pCLAMP software (Axon Instruments, Foster City, CA).

[^{125}I]-α-Bungarotoxin (α-Bgt) Binding Assays. Total surface expression of α-Bgt binding sites was tested with 5 nM [^{125}I]-α-Bgt as described (García-Guzmán et al., 1994). All binding assays were performed in individual oocytes. For displacement experiments, oocytes were incubated with 1 nM (α7 WT) or 10 nM (C28) α-Bgt in the presence of increasing concentrations of nicotine.

Data Analysis. Current amplitudes were measured at the peak inward current, and no correction for desensitization was made. Dose−response curves were fitted using a nonlinear least-squares algorithm to the Hill equation, $I/I_{max} = 1/[1 + (EC_{50}/C)^h]$, where EC_{50} is the agonist concentration which elicits the half-maximal response, h is the Hill coefficient, and C is the agonist concentration. Statistical significance was calculated by a Student's t test or nonparametric Mann−Whitney test.

Computer Simulations. Kinetic model simulations were performed using the techniques described by Colquhoun and Hawkes (1995) and implemented in MathCad Plus 6.0 software (MathSoft Inc., Cambridge, MA). The multidimensional minimization routine AMOEBA (Press et al., 1992) was used to find the value of the kinetic constants that fitted the observed data: maximal current (I_{max}) and decay half-time for the currents and EC_{50} for the dose−response curves.

RESULTS AND DISCUSSION

The use of chimeric receptors has been helpful in understanding the relationships between structure and function in AChRs (Luetje et al., 1993; Eiselé et al., 1993; Figl et al., 1996). Moreover, chimeric receptors have been useful in the assignment of functional roles to different domains in both voltage-dependent and ligand-gated ion channels. The present study originated from the finding that two α7/α3 chimeric receptors, C10 and C21 (Figure 1), have been shown to be able to form functional receptors when expressed in *Xenopus* oocytes (Campos-Caro et al., 1996), but their kinetics showed important differences with respect to α7 wild type receptors (WT) (Figure 2). These two chimeric subunits contain the α7 sequence from the N terminus to the beginning of the putative transmembrane segment M3 and the α3 sequence from there to the C terminus. To investigate which domains would be involved in such changes, we constructed an additional series of chimeric α7/α3 subunits, some of which were able to form functional receptors. Domains studied are depicted in Figure 1.

Since the nicotine-evoked currents measured in the oocytes are dependent on both the extent of AChR expression and its sensitivity to agonists, we normalized the ionic currents obtained upon stimulation with high concentrations of agonists (established after the study of the dose−response relationships, Table 1) to the expression of α-Bgt binding sites in the membrane of each individual oocyte. As long as all chimeras share the same sequence at the N-terminal domain, where the α-Bgt binding site is thought to be, we assumed that α-Bgt binding was similar in all of them (for a detailed discussion on the value of the estimates, see below). After this normalization procedure, all expressed chimeras showed: (i) a decrease in the I_{max} evoked by nicotine, (ii) a decrease in the rate of macroscopic desensitization upon stimulation with nearly saturating concentrations of nicotine, and (iii) a decrease in the EC_{50} for ACh and nicotine (Figure 2 and Table 1).

After the analysis of these chimeras, several conclusions could be drawn. For instance, C10 and C21 showed differences between them, in spite of differing in only two residues (domain A). But unlike mutations of neighboring residues (Campos-Caro et al., 1996), neither C32 nor the single-point mutations at the two locations (not shown) gave receptors that differed significantly from WT (Figure 2 and Table 1). According to this, the differences observed between C10 and C21 would probably arise from the interaction of the domain A with other residues of the α3 sequence that are present in C10 and C21.

Also, it has been demonstrated that a residue in the M4 domain of the *Torpedo* α subunit (αCys418) influences AChR function (Lee et al., 1994). Although our chimeras contain much broader changes than a point mutation, it is

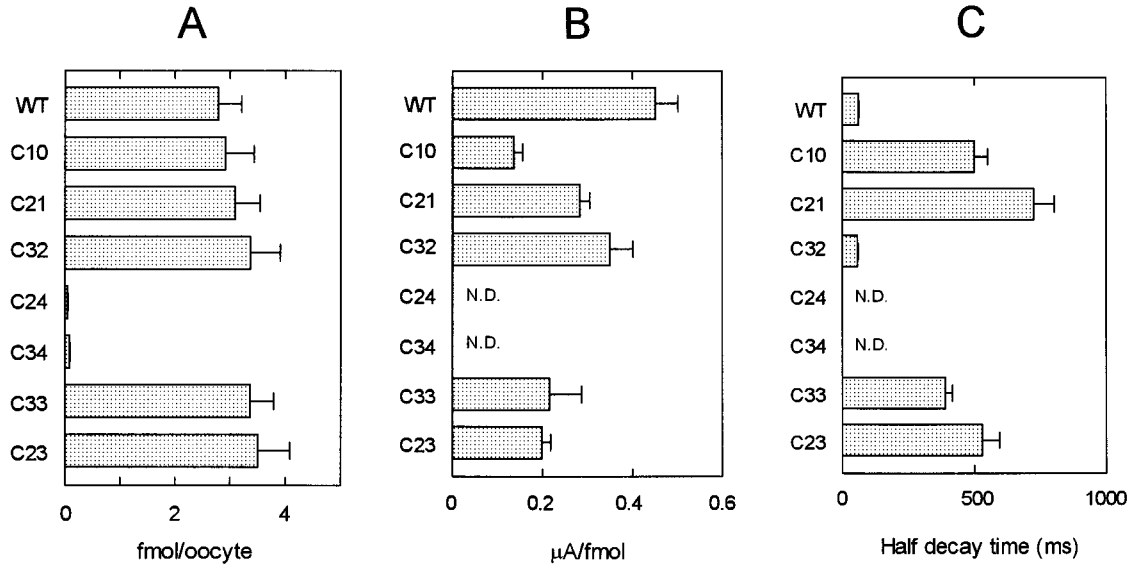

FIGURE 2: Functional parameters of α7 and chimeric receptors. (A) Surface expression of α-Bgt binding sites. (B) Mean maximal currents upon stimulation with nicotine. Inward currents were obtained at −40 mV (250 μM for WT and C32 and 50 μM nicotine for all other chimeras) and then divided by the value obtained in the binding measurement for the same oocyte, as in panel A. (C) Desensitization rate measured as the decay half-time of maximal inward currents measured as in panel B. Data are means with SEM of 20−50 individually measured oocytes from three to five donors. N. D. represents not determined. All differences with respect to WT in panels B and C were statistically significant ($p < 0.01$), except for C32.

Table 1: Apparent Affinity of Wild Type and Chimeric α7 Receptors for Two Different Nicotinic Agonists[a]

	acetylcholine			nicotine		
receptor	EC_{50}	h	$(n, d)^b$	EC_{50}	h	$(n, d)^b$
WT	59 ± 8	1.51	(9, 3)	39 ± 3	1.72	(11, 3)
C10	8.5 ± 3.1	1.46	(9, 4)	3.3 ±1.3	1.14	(10, 3)
C21	5.0 ± 2.1	1.45	(8, 4)	1.5 ± 0.3	1.54	(14, 3)
C32	63 ± 14	1.99	(7, 3)	51 ± 7	1.85	(7, 2)
C33	5.8 ± 0.8	2.45	(9, 3)	4.7 ± 2.3	1.10	(7, 3)
C23	6.6 ± 1.2	1.81	(9, 3)	3.5 ± 1.0	1.33	(10, 2)
C28	8.3 ± 2.5	1.01	(8, 3)	6.8 ± 1.0	1.30	(11, 3)

[a] Data were fitted by the Hill equation (see Materials and Methods). Values are mean ± SEE (micromolar). [b] n is the number of oocytes; d is the number of donors.

worth noting that the cysteine residue mentioned above is present at the equivalent position in the neuronal α3 subunit (and also C10 and C21), but not in the α7 subunit (nor C33 or C23). Comparison of these four chimeras among them suggests a possible role of the M4 domain (and/or the C-terminal domain); however, they are not consistent with the findings of Lee and co-workers, probably due to the more extensive changes present in our chimeras. In any case, if C23 and C33 receptors were compared with WT, the three differences mentioned above were still detected: smaller currents, slower desensitization, and a smaller EC_{50} (Figure 2 and Table 1). Therefore, a critical role of the M4 domain in the induction of these three effects can be discarded.

All chimeras tested so far shared the α3 sequence in both the transmembrane segment M3 and the large intracellular loop between M3 and M4 (domains B and C). In order to test the contribution of M3 to the observed effects, we swapped the M3 segment of α7 with the one corresponding to α3 (domain B), as in C28. Table 1 shows that the dose−response relationships for both nicotine and ACh are also shifted to the left almost 1 order of magnitude in C28 with respect to WT. Moreover, maximal currents were smaller, and also, the rate of macroscopic desensitization was slower (Figure 3). Therefore, the swapping of only the M3 domain (C28) led to the same qualitative features shared by all other chimeras. The results obtained with C28 also argue against a crucial role of the large intracellular M3−M4 loop (domain C) in the kinetic behavior of the previous chimeras. Particularly, it is important to indicate that domain C contains putative phosphorylation sites for different protein kinases [for a complete comparison of the sequences, see Criado et al. (1992) and García-Guzmán et al. (1995)]. For instance, a PKA-dependent phosphorylation site has been removed in most chimeras. This site could be most likely phosphorylated in WT receptors (Hoffman et al., 1994), so its removal could have decreased the desensitization rate (Huganir et al., 1986; Hopfield et al., 1988; Hoffman et al., 1994). However, this is probably not the mechanism involved in the reduction of the desensitization rate, because C28 receptors exhibited the slowest macroscopic desensitization rates, in spite of preserving the PKA-dependent phosphorylation sites present in WT. Whatever the case, an independent effect of this domain on the desensitization of α7 receptors could not be discarded, since neither a chimeric subunit including the α3 sequence only in domain C nor point mutants at the putative phosphorylation sites of WT have been made in this study.

In summary, all the differences mentioned above between WT and chimeric receptors may be mostly attributed to the M3 domain.

It should be pointed out that all values of α-Bgt binding sites have been obtained after incubations with 5 nM α-Bgt. Since C28 presented a smaller affinity for α-Bgt (Figure 4; see below for discussion), 5 nM is a nonsaturating concentration and should underestimate the total number of C28 receptors. Although the reduction in I_{max} is also clear without correction, the numbers shown in Figure 3 (but not those of Figure 2) have been corrected to account for this bias. It is also worth noticing the larger expression of α-Bgt binding sites in this series, when compared with that of Figure 2 (more than 2-fold). This is probably due to the fact that the cRNAs used in this series originated in a different synthesis (C21 expression in the latter series was also enhanced by

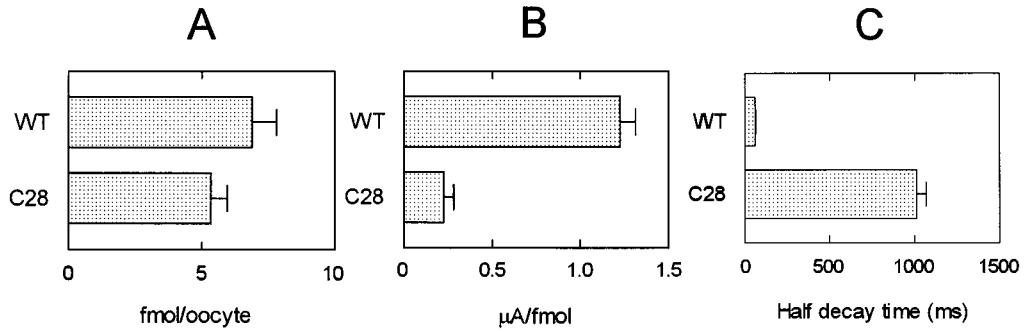

FIGURE 3: Functional parameters of α7 and chimeric C28 receptors. (A) Surface expression of α-Bgt binding sites. Data of C28 chimeric receptors have been multiplied by a factor of 3.4 to account for the nonsaturating concentration of α-Bgt used in the incubation (see the text for an explanation). (B) Mean maximal currents upon stimulation with nicotine. Inward currents were obtained at −80 mV (250 μM for WT and 50 μM nicotine for C28) and then divided by the corrected value obtained in the binding measurement for the same oocyte, as in panel A. (C) Desensitization rate measured as the decay half-time of maximal inward currents measured as in panel B. Data are means with SEM of 60−66 (A and B) and 25−56 (C) individually measured oocytes from five donors. Differences were statistically significant in panels B and C ($p < 0.001$).

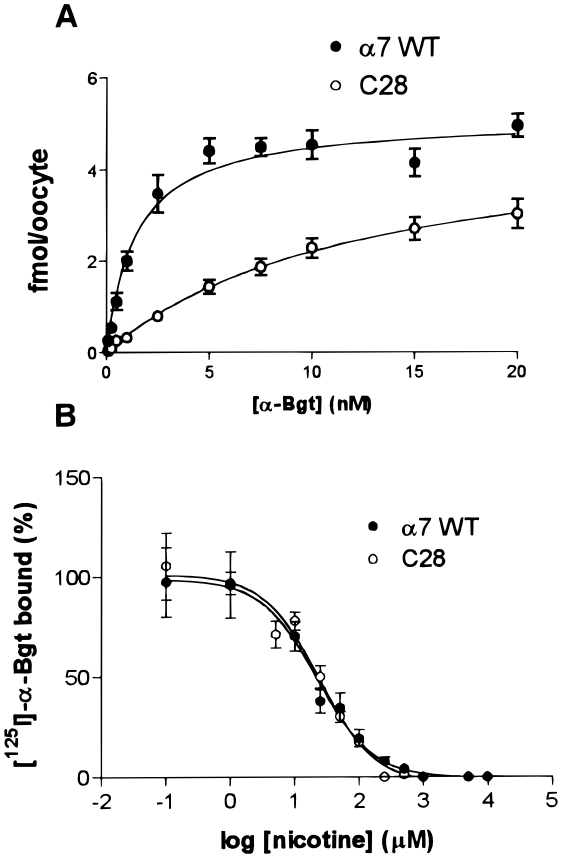

FIGURE 4: Binding properties of α7 and C28 receptors expressed in Xenopus oocytes. (A) Saturation curves of α-Bgt binding to oocytes. Each point represents the mean with SEM of binding to 10−20 oocytes (two or three donors). B_{max} values were 5.1 and 4.9 fmol per oocyte, and K_d values were 1.4 ± 0.3 and 12.0 ± 0.7 nM for α7 and C28 receptors, respectively. (B) Nicotine displacement curves of bound α-Bgt from oocyte membranes expressing α7 and C28 receptors. Data represent the mean with SEM of 7−25 oocytes (one or two donors). Continuous lines represent fits to the Hill equation ($h = -1$) with IC_{50} values of 22 and 24 μM (K_i values of 12.8 and 13.0 μM) for α7 and C28 receptors, respectively.

the same factor; not shown).

Reduction of Ionotropic Responses. The decrease in the magnitude of the maximal currents evoked by nicotinic agonists could have been due to several mechanisms.

(a) The possibility that chimeric receptors presented a smaller proportion of functional channels could not be fully discarded, but sucrose gradient centrifugation gave unique molecular species with sizes close to that of *Torpedo* AChR monomers, indicating that all chimeric receptors assembled in pentamers (not shown).

(b) Reduced expression of chimeric receptors in the oocyte system has been considered because values of I_{max} are normalized to the estimated number of surface receptors, as measured by α-Bgt binding sites. Moreover, values of normalized maximal currents evoked by nicotine in chimeric receptors may be overestimated, as all binding experiments shown in Figures 2 and 3 were done with 5 nM α-Bgt, as mentioned above. Another point to consider is that maximal currents were estimated as the peak current measured at high agonist concentrations where desensitization or open channel block could occur, thus distorting the estimates. But again, the more distorted measurements would be those in currents displaying faster desensitization, as WT receptors, which then would be underestimated. Therefore, correcting the maximal currents to account for desensitization would give even greater reductions in the maximal currents obtained in slow desensitizing chimeras.

(c) Another explanation which would account for smaller I_{max} values could be the existence of modifications in the elementary conductances of chimeric receptors. Since we have not been able to obtain single-channel recordings of α7 receptors, this possibility cannot be fully discarded at present. However, all reported changes in single-channel conductance have been produced by modifications of residues within or near the M2 segment, which putatively lines the ionic pore of all LGICs (Leonard et al., 1988; Imoto et al., 1988), and this is not the case in any of the chimeras presented here.

(d) Finally, assuming that the above explanations are unlikely to explain the reduction in maximal currents, it is strongly suggested that the chimeric receptors have changed their gating behavior due to the presence of the α3 sequence at the M3 domain.

Kinetic Modeling. Markovian models provide a reasonable and well-accepted basis for describing the kinetic properties of ion channels. Thus, the functional properties of the C28 receptors might be interpreted in terms of changes in the rate constants of kinetic schemes of AChRs. By means of computer simulations, we tried to find out what changes in kinetic rate constants could account for the features of C28. We used a simple kinetic scheme consisting of five states. In such a scheme, AChR binds two molecules of agonist

(state L_2R), and then the channel opens (state L_2O). Also, the desensitized state (L_2D) is fully coupled to opening of the channels.

$$R \underset{k_{-1}}{\overset{2\cdot k_1}{\rightleftharpoons}} LR \underset{2\cdot k_{-1}}{\overset{k_1}{\rightleftharpoons}} L_2R \underset{\alpha}{\overset{\beta}{\rightleftharpoons}} L_2O \underset{d_{-1}}{\overset{d_1}{\rightleftharpoons}} L_2D$$

First, we run simulations to match the main electrophysiological and pharmacological properties of WT receptors (I_{max}, desensitization kinetics, and EC_{50}). The value of the maximal open probability was set at 0.01, by assuming that one receptor binds five molecules of α-Bgt and that the single-channel conductance is 45 pS (Revah et al., 1991). Constraints included in the model were as follows: $k_1 = 10$ μM^{-1} s^{-1} [similar to that obtained for the competitive antagonist methyllycaconitine in α7 receptors by Palma et al. (1996)] and $d_{-1} = 0.005$ s^{-1} (to fit the time course of the recovery from desensitization after 3 s of continuous application of 250 μM nicotine; our unpublished data). Simulations of the WT features could be achieved by a number of combinations of the remaining parameters, but the most sensitive ones were β and d_1 for matching both, I_{max} and the desensitization rate, and k_{-1} for obtaining the EC_{50}. On the other hand, for an $\alpha < 500$ s^{-1}, large changes in α could be compensated by very small changes in β; thus, we fixed the value of α to 500 s^{-1}, and the features of WT receptors can be fairly reproduced with the values shown in Figure 5A. It is worth noting that, in order to match both I_{max} and the decay half-time, the desensitization kinetics should be rate limited by the slow activation rate β.

Then, we tried to simulate the behavior of C28 receptors by changing a single rate constant at a time. We found that, in order to match both the smaller I_{max} and the slower desensitization kinetics, a double change in d_1 (2-fold decrease) and in either α (20-fold increase) or β (11-fold decrease) was needed (Figure 5B, solid line). Nevertheless, the construction of a dose-response curve from currents simulated by the latter set of kinetic constants gave estimates of nicotine's EC_{50} of around 37 μM, which significantly differed from that obtained experimentally for C28 (Figure 5C, symbols and thick solid line).

Usually, when the maximal current decreases because of a reduction of the β/α ratio, the measured value of EC_{50} should increase or remain unchanged (Amin & Weiss, 1993). That is what happened if the simulations, which reproduced the kinetics, were run with "high" values for binding rates. Then, to obtain a dose−response curve similar to that of C28, it was necessary to include an additional change in the value of the backward binding rate, k_{-1} (Figure 5C, fine solid line). If this has really happened in C28 receptors, it would suggest an effect of M3 on binding rates, making necessary the postulation that either the M3 domain is part of the agonist binding site or the effect of substituting the M3 domain involves a great change in the overall configuration of C28 with respect to WT that could affect the agonist binding site. The first explanation seems unlikely because the M3 domain is thought to be inserted in the plasma membrane, far from the putative binding site (Unwin, 1995; Karlin & Akabas, 1995), but the latter is very difficult to discard in any substitution experiments. Concerning this point, C28 recep-

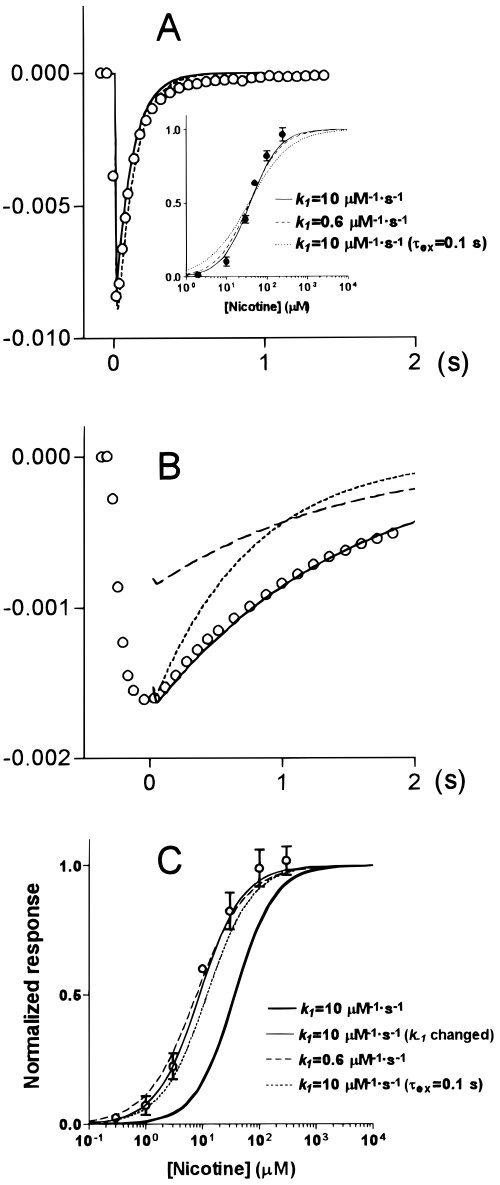

FIGURE 5: Computer simulations of currents and dose−response curves. (A) (○) α7 ionic current produced by the application of 250 μM nicotine. Data have been scaled to represent the fraction of open channels; see the text for details. (—) Model prediction with the following set of kinetic constants (set a): $k_1 = 10$, $k_{-1} = 150$, $\beta = 16$, $\alpha = 500$, $d_1 = 1000$, $d_{-1} = 0.005$ (in μM^{-1} s^{-1} for k_1 and s^{-1} for the rest). (− −) Model prediction with set b of kinetic constants (changes with respect to set a were $k_1 = 0.6$, and $k_{-1} = 1$). (Inset) Dose−response curve for α7 receptors. (●) Data points with standard errors. (—) Model prediction with set a of kinetic constants ($EC_{50} = 37.8$ μM; $h = 1.22$). (− −) Identification with set b ($EC_{50} = 36$ μM; $h = 1.06$). (···) Model prediction with set c of kinetic constants (change with respect to set a was $k_{-1} = 42$), in which agonist applications follow a monoexponential time course with $\tau_{ex} = 0.1$ s ($EC_{50} = 35$ μM; $h = 0.84$). (B) (○) Current data from C28 produced and scaled as in panel A. (—) Model prediction obtained by changing both $\beta = 1.6$ and $d_1 = 484$ to set a. (− −) Identification by changing only $\beta = 1.2$ which matched the desensitization time course. (···) Identification by changing only $\beta = 2.4$ which matched the I_{max}. (C) Dose−response curve for C28. (○) Data points with standard errors. (Thick —) Model prediction obtained by changing β and d_1 as in panel B ($EC_{50} = 37$ μM; $h = 1.25$). (Fine —) Model prediction obtained by changing $k_{-1} = 36$, $\beta = 1.5$, $d_1 = 447$ to set a ($EC_{50} = 8.8$ μM; $h = 1.15$). (− −) Model prediction obtained by changing $\beta = 1.5$ and $d_1 = 450$ to set b ($EC_{50} = 7.8$ mM; $h = 1.05$). (···) Model prediction obtained by changing $\beta = 1.5$ and $d_1 = 450$ to set c ($EC_{50} = 12$ μM; $h = 1.10$).

tors presented changes in the affinity for α-Bgt (Figure 4A), but on the other hand, experiments displacing α-Bgt by nicotine showed an almost identical affinity for nicotine (Figure 4B). Due to the differences in size between α-Bgt and nicotine, these results suggest that the M3 substitution alters the major structure of the extracellular part of the receptor, modifying some of the many α-Bgt anchoring sites, but leaving the agonist binding site unaffected.

Curiously, if the simulations of WT started to be constrained by a smaller value of k_1 (0.6 μM^{-1} s^{-1}), then all parameters measured in C28 can be simulated only by changes in gating rate constants, the β/α ratio and d_1 (Figure 5C, dashed line). However, the presence of desensitization forces the EC_{50} value to be determined by a very complex interplay among all kinetic rate constants. Moreover, it is likely that our measurements were rate limited by the large size of the oocytes. If a diffusional delay in the arrival of the agonist ($\tau_{ex} = 100$ ms) for both WT and C28 receptors is included in the model, then the shift to the left in the EC_{50} is also simulated without changing binding rates (Figure 5C, dotted line). This would suggest that shifts to the left in dose−response curves might be due to an "effective" forward binding rate slower than the actual one. With all these eventualities taken together, we favor the case in which the substitution of the M3 domain in neuronal nicotinic AChRs would not affect their agonist binding properties, as displacement experiments also suggested (Figure 4B). However, the accurate determination of the values taken by the agonist binding rates, though difficult to achieve (Changeux & Edelstein, 1994), would be the only way to ascertain or discard this conclusion.

To check the strength of our conclusions, we have used other kinetic models (not shown). For instance, we have included an additional kinetic state connected to the open state in order to simulate the presence of agonist open channel block. However, the use of rate constants similar to those reported by Mathie et al. (1991) also required changes of the same magnitude in the β/α ratio, i.e. an 18-fold reduction of β. Likewise, the use of other kinetic models where desensitization is allowed to occur from closed states, including the allosteric model, still required changes in the β/α ratio, which according to Galzi et al. (1996) would correspond to an L phenotype. Alternatively, the use of the allosteric model might predict the kinetics of C28 receptors if equilibria between kinetic states were altered in a weird manner, i.e. toward desensitized states in unoccupied receptors and toward activatable or active states in liganded receptors. In summary, regardless of the kinetic model used, the binding rate values, or the velocity of solution exchange, an identical change in the β/α ratio is the simplest way to simulate the kinetics of C28 receptors and, therefore, stressing the main conclusion that the presence of the M3 segment affects the gating of the α7 receptors.

The available data do not allow the detailed kinetic modeling that single-channel measurements would. Unfortunately, in spite of trying with oocytes expressing large macroscopic currents, and probably due to a clustered distribution of receptors (Revah et al., 1991), we have not been able to obtain single-channel records of α7-like receptors.

There is much evidence in favor of the effect of many amino acid substitutions on binding and/or gating of LGICs, including residues located at the N-terminal domain, the M1 domain, the M2 domain, the M2−M3 loop, and the M4 domain [see the introductory section for specific references; more recently reviewed by Karlin and Akabas (1995)]. Here we have presented evidence of the effect on gating properties of neuronal AChRs after substitutions in another area, the putative transmembrane M3 domain. According to recent structural and mutational studies, a well-conserved leucine residue located at the middle of the M2 segment, presumably at the kink of the α-helix (Unwin, 1995), could govern the gating of AChRs, although there is not strong evidence in favor of these residues actually forming the gate (Filatov & White, 1995; Labarca et al., 1995). After rotation of the M2 α-helices, these leucine residues might interact with other residues, perhaps located in the M3 domain. Alternatively, cysteine substitution experiments have shown that the gate of mouse muscle AChRs is much farther down the channel than the mentioned leucines (Akabas et al., 1994), making likely the possibility that the gate could be formed by residues in the loop between M3 and M4 (Karlin & Akabas, 1995), some of which have been swapped in C28 (see the bottom of Figure 1).

Site-directed mutagenesis experiments have shown that the functional properties of the pore seem to be almost exclusively determined by residues located in or near the M2 domain [but see Akabas and Karlin (1995)]. In contrast, the present study adds to a series of reports showing that the gating properties of AChR channels are affected by modifications in many areas of the molecule, suggesting that a large number of residues are involved in the gating mechanism. An alternative explanation is that the structure of the channel gate itself could be much simpler, but strongly dependent on the overall structure of the receptor.

Our study does not provide evidence about the mechanism (changes in α or β) by which the M3 substitution affects the gating of AChRs. Either mechanism makes very distinguishable predictions in microscopic kinetics, and therefore, single-channel data, perhaps from other AChRs more suitable for recording elementary currents, should be obtained to solve this question.

REFERENCES

Adams, P. R. (1975) *Pfluegers Arch. 360*, 133−144.

Akabas, M. H., & Karlin, A. (1995) *Biochemistry 34*, 12496−12500.

Akabas, M. H., Stauffer, D. A., Xu, M., & Karlin, A. (1992) *Science 258*, 307−310.

Akabas, M. H., Kaufmann, C., Archdeacon, P., & Karlin, A. (1994) *Neuron 13*, 919−927.

Amin, J., & Weiss, D. S. (1993) *Nature 366*, 565−569.

Aylwin, M. L., & White, M. M. (1994) *Mol. Pharmacol. 46*, 1149−1155.

Campos-Caro, A., Sala, S., Ballesta, J. J., Vicente-Agulló, F., Criado, M., & Sala, F. (1996) *Proc. Natl. Acad. Sci. U.S.A. 93*, 6118−6123.

Changeux, J. P., & Edelstein, S. J. (1994) *Trends Biochem. Sci. 19*, 399−400.

Chen, J., Zhang, Y., Akk, G., Sine, S., & Auerbach, A. (1995) *Biophys. J. 69*, 849−859.

Colquhoun, D., & Hawkes, A. G. (1995) in *Single Channel Recording* (Sakmann, B., & Neher, E., Eds.) pp 589−633, Plenum Press, New York.

Criado, M., Alamo, L., & Navarro, A. (1992) *Neurochem. Res. 17*, 281−287.

Edmonds, B., Gibb, A. J., & Colquhoun, D. (1995) *Annu. Rev. Physiol. 57*, 469−493.

Eiselé, J. L., Bertrand, S., Galzi, J.-L., Devillers-Thiéry, A., Changeux, J.-P., & Bertrand, D. (1993) *Nature 366*, 479−483.

Figl, A., Labarca, C., Davidson, N., Lester, H. A., & Cohen, B. N. (1996) *J. Gen. Physiol. 107*, 369−379.
Filatov, G. N., & White, M. M. (1995) *Mol. Pharmacol. 48*, 379−384.
Galzi, J.-L., Devillers-Thiéry, A., Hussy, N., Bertrand, S., Changeux, J.-P., & Bertrand, D. (1992) *Nature 359*, 500−505.
Galzi, J.-L., Edelstein, S. J., & Changeux, J.-P. (1996) *Proc. Natl. Acad. Sci. U.S.A. 93*, 1853−1858.
García-Guzmán, M., Sala, F., Sala, S., Campos-Caro, A., & Criado, M. (1994) *Biochemistry 33*, 15198−15203.
García-Guzmán, M., Sala, F., Sala, S., Campos-Caro, A., Stühmer, W., Gutiérrez, L. M., & Criado, M. (1995) *Eur. J. Neurosci. 7*, 647−655.
Herlitze, S., & Koenen, M. (1990) *Gene 2*, 66−68.
Hoffman, P. W., Ravindran, A., & Huganir, R. L. (1994) *J. Neurosci. 14*, 4185−4195.
Hopfield, J. F., Tank, D. W., Greengard, P., & Huganir, R. L. (1988) *Nature 336*, 677−680.
Huganir, R. L., Delcour, A. H., Greengard, P., & Hess, G. P. (1986) *Nature 321*, 774−776.
Imoto, K., Busch, C., Sakmann, B., Mishina, M., Konno, T., Nakai, J., Bujo, H., Mori, Y., Fukuda, K., & Numa, S. (1988) *Nature 335*, 645−648.
Karlin, A., & Akabas, M. H. (1995) *Neuron 15*, 1231−1244.
Krieg, P. A., & Melton, D. A. (1984) *Nucleic Acids Res. 12*, 7057−7070.
Labarca, C., Nowak, M. W., Zhang, H., Tang, L., Deshpande, P., & Lester, H. A. (1995) *Nature 376*, 514−516.
Lee, Y. H., Li, L., Lasalde, J., Rojas, L., McNamee, M., Ortiz-Miranda, S. I., & Pappone, P. (1994) *Biophys. J. 66*, 646−653.
Leonard, R. J., Labarca, C. G., Charnet, P., Davidson, N., & Lester, H. A. (1988) *Science 242*, 1578−1581.
Lo, D. C., Pinkham, J. L., & Stevens, C. F. (1991) *Neuron 6*, 31−40.
Luetje, C. W., Piattoni, M., & Patrick, J. (1993) *Mol. Pharmacol. 44*, 657−666.
Mathie, A., Cull-Candy, S. G., & Colquhoun, D. (1991) *J. Physiol. 439*, 717−750.
McGehee, D. S., & Role, L. W. (1995) *Annu. Rev. Physiol. 57*, 521−546.
McLaughlin, J. T., Hawrot, E., & Yellen, G. (1995) *Biochem. J. 310*, 765−769.
O'Leary, M. E., & White, M. M. (1992) *J. Biol. Chem. 267*, 8360−8365.
Palma, E., Bertrand, S., Binzioni, T., & Bertrand, D. (1996) *J. Physiol. 491*, 151−161.
Papke, R. L. (1993) *Prog. Neurobiol. 41*, 509−531.
Press, W. H., Teukolsky, S. A., Vetterling, W. T., & Flannery, B. P. (1992) in *Numerical Recipes in C*, Cambridge University Press, Cambridge.
Rajendra, S., Lynch, J. W., Pierce, K. D., French, C. R., Barry, P. H., & Schofield, P. R. (1995) *Neuron 14*, 169−175.
Revah, F., Bertrand, D., Galzi, J.-L., Devillers-Thiéry, A., Mulle, C., Hussy, N., Bertrand, S., Ballivet, M., & Changeux, J.-P. (1991) *Nature 353*, 846−849.
Séguéla, P., Wadiche, J., Dineley-Miller, K., Dani, J. A., & Patrick, J. W. (1993) *J. Neurosci. 13*, 596−604.
Unwin, N. (1995) *Nature 373*, 37−43.

BI9623486